# Hetero-Grafted Block Brushes with PCL and PBA Side Chains

**Hyung-il Lee,[†] Krzysztof Matyjaszewski,*[,†] Sherryl Yu-Su,[‡] and Sergei S. Sheiko[‡]**

*Center for Macromolecular Engineering, Department of Chemistry, Carnegie Mellon University, 4400 Fifth Avenue, Pittsburgh, Pennsylvania 15213, and Department of Chemistry, University of North Carolina at Chapel Hill, Chapel Hill, North Carolina 27599-3290*

*Received February 23, 2008; Revised Manuscript Received June 9, 2008*

ABSTRACT: Giant amphiphilic macromolecules, hetero-grafted block brushes with a crystalline poly(ε-caprolactone) (PCL) brushlike block and an amorphous poly(*n*-butyl acrylate) (PBA) brush as the second block, were synthesized entirely by the "grafting from" approach using a combination of atom transfer radical polymerization (ATRP) and ring-opening polymerization (ROP). The following steps were employed for the preparation of the brush: (1) A well-defined poly(2-hydroxyethyl methacrylate) (PHEMA) was synthesized by ATRP. (2) PHEMA was used as a macroinitiator for chain extension with 2-(trimethylsilyloxy)ethyl methacrylate (HEMATMS) via ATRP to provide PHEMA-*b*-PHEMATMS. (3) The hydroxyl groups of PHEMA were transformed to bromoisobutyryl ATRP initiating groups to give poly[{2-(2-bromoisobutyryloxy)ethyl methacrylate}-*block*-(HEMATMS)], PBiBEM-*b*-PHEMATMS. (4) PBiBEM-*b*-PHEMATMS was transformed to PBiBEM-*b*-PHEMA by treatment with tetrabutylammonium fluoride (TBAF) in THF. (5) PCL was grafted from the PBiBEM-*b*-PHEMA macroinitiator by ROP in the presence of tin(II) 2-ethylhexanoate ($Sn(EH)_2$) catalyst. (6) The PBA chains were grafted from the brush macroinitiators by ATRP. Molecular weight, molecular weight distribution, and the degree of polymerization (DP) of the backbone and the PBA and PCL side chains were determined by gel permeation chromatography (GPC) and $^1$H NMR spectroscopy. Thermal transition of the hetero-grafted block brush was investigated by differential scanning calorimetry (DSC). Molecular imaging by atomic force microscopy was used to verify the success of the synthetic strategy for this complex molecule. Because of their amphiphilic structure, the hetero-grafted diblock brushes demonstrated association into flower-like or dumbbell-like structures.

## Introduction

Bottle-brush macromolecules are single graft copolymer molecules with a well-defined cylindrical shape which is a result of the steric hindrance and excluded volume repulsion between densely grafted side chains attached to a flexible polymer backbone.[1–6] Recently, considerable attention has been drawn to brush macromolecules due to their potential for intramolecular nanoengineering, such as templates for inorganic nanoparticles or nanowires,[7–9] and for development of novel material properties, such as supersoft elastomers.[10,11]

The establishment of facile controlled radical polymerization methods such as atom transfer radical polymerization (ATRP)[12–17] allows for complete control/design of the molecular architecture of brushes, producing unique and novel molecules such as starlike multiarm structures,[18,19] cylindrical brush−coil block copolymers,[20,21] AB-type brush-*block*-brush copolymers,[22] brushes with block copolymer side chains,[23–26] and brushes with a gradient in grafting density along the copolymer backbone.[27–29] Ring-opening polymerization (ROP)[30–32] has been also used to prepare molecular brushes with crystallizable side chains. This technique is particularly attractive since it operates with fundamentally different polymerization mechanism, which provides a convenient way to prepare copolymers with different architectures and compositions when used in conjunction with ATRP.

Among the architectural possibilities for brush macromolecules, hetero-grafted block brushes have not been studied extensively due to limited synthetic approaches. For instance, Ishizu et al.[22] prepared the hetero-grafted block brushes by combination of the "grafting through"[4,33–37] (polymerization of macromonomers) and "grafting from"[1,24,38–40] (polymerization of monomers from the macroinitiator backbone) techniques. However, this pioneering approach has some shortcomings. First, it was difficult to achieve a high DP during the polymerization of a macromonomer due to their steric strain in propagation (step 1 in Scheme 1A). Second, the removal of excess macromonomers to isolate the pure brush copolymer was challenging. Third, chain extension from the brush macroinitiator to give brush-*block*-coil (step 2 in Scheme 1A) was inefficient because of the steric congestion around the initiating site at the end of the backbone.

An alternative way for preparing hetero-grafted block brushes is to conduct a "grafting from" technique throughout the whole procedure. To accomplish this, a block copolymer backbone with two different initiating sites that can subsequently grow two distinct side chains sequentially from the appropriate initiating sites should be prepared (Scheme 1B).

In this article, we demonstrate, for the first time, the successful synthesis of the hetero-grafted block brushes with poly(ε-caprolactone) (PCL) and poly(*n*-butyl acrylate) (PBA) side chains using only the "grafting from" technique. The crystalline PCL was synthesized by ROP from a poly[{2-(2-bromoisobutyryloxy)ethyl methacrylate}-*block*-(2-hydroxyethyl methacrylate)] (PBiBEM-*b*-PHEMA) block copolymer backbone. Then, the amorphous PBA segments were synthesized by ATRP to give the hetero-grafted block brush, (PBiBEM-*g*-PBA)-*b*-(PHEMA-*g*-PCL). The success of the synthetic strategy for this complex hetero-grafted PBA brush-*block*-PCL brush copolymer was verified through imaging of individual molecules by AFM.[41–45]

## Experimental Section

**Materials.** 2-(Trimethylsilyloxy)ethyl methacrylate (HEMATMS) (99%) was purchased from Polysciences. 2-Hydroxyethyl methacrylate (HEMA) and *n*-butyl acrylate were purchased from Acros and distilled under vacuum prior to use. ε-Caprolactone (99%), ethyl 2-bromoisobutyrate (98%) (EBiB), 2-bromo-2-methylpropionic acid (98%), 4,4′-di(5-nonyl)-2,2′-bipyridine (dNb-

* Corresponding author. E-mail: km3b@andrew.cmu.edu.
† Carnegie Mellon University.
‡ University of North Carolina at Chapel Hill.

10.1021/ma800412s CCC: $40.75 
Published on Web 07/22/2008

**Scheme 1. (A) Preparation of the Hetero-Grafted Block Brushes by Combination of "Grafting Through" and "Grafting From" Techniques;[a] (B) Preparation of the Hetero-Grafted Block Brushes by the Entire "Grafting From" Technique**

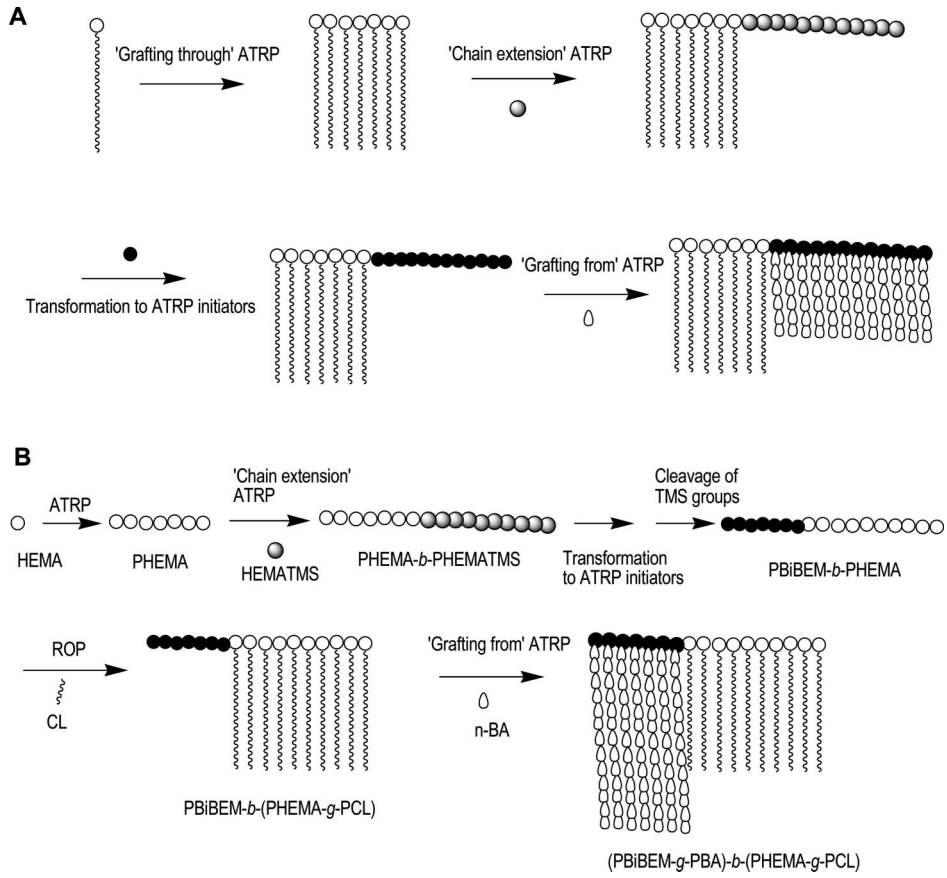


[a] The polymerization of methacryloyl-terminated poly(ethylene glycol methyl ether) macromonomer (PEG-MC) using the ATRP "grafting through" technique was followed by subsequent ATRP of 2-hydroxyethyl methacrylate (HEMA) from this brush macroinitiator to give PEG brush-*block*-PHEMA (brush-*block*-coil) diblock copolymers. Esterification of the pendant hydroxyl groups in the PHEMA block with 2-bromoisobutyryl bromide yields a block-type multi-initiator, brush-*block*-poly(2-(2-bromoisobutyryloxy)ethyl methacrylate) (PBIEM). ATRP of HEMA using the brush-*block*-PBIEM as a polyinitiator provided AB-type brush-*block*-brush amphiphilic copolymers.

**Scheme 2. Synthesis of the Hetero-Grafted Block Brushes Containing PCL and PBA Side Chains**

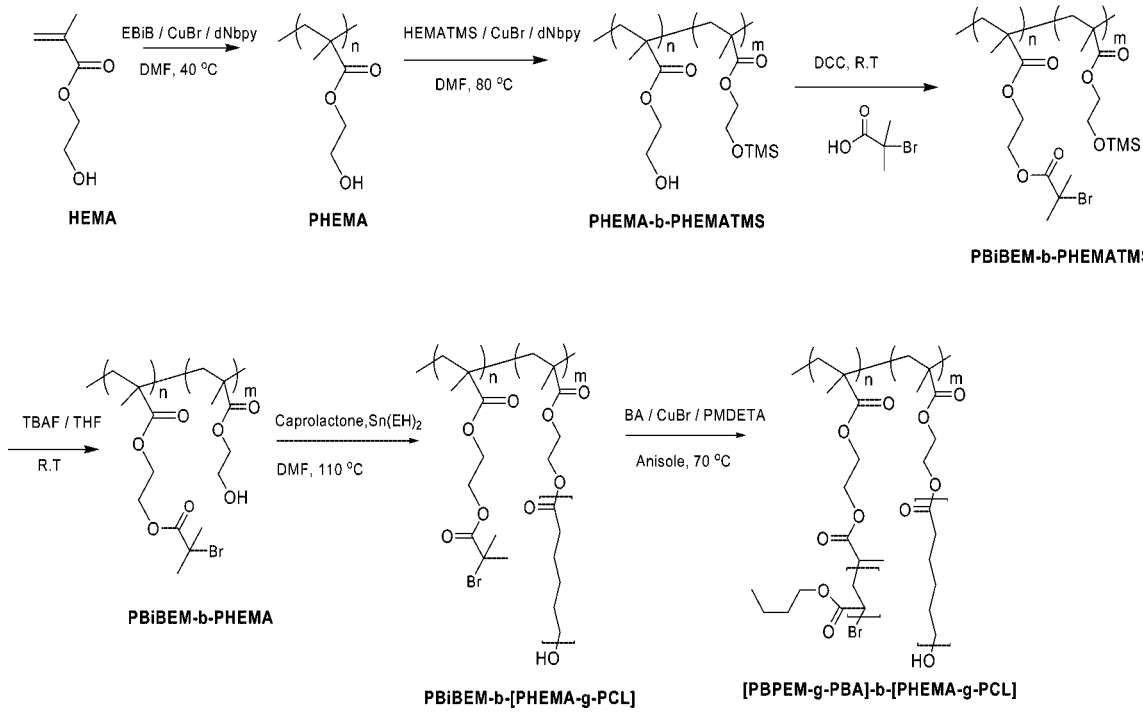

py),[46,47] *N,N′*-dicyclohexylcarbodiimide (DCC) (99%), dimethylformamide (DMF) (extra dry, less than 50 ppm of water), 1 M tetrabutylammonium fluoride (TBAF) in THF, and tin(II) 2-ethylhexanoate ($Sn(EH)_2$) were purchased from Aldrich Chemical Co. ε-Caprolactone (CL) (Aldrich, 99%) was dried over calcium hydride under nitrogen at 25 °C, distilled under reduced pressure, and stored over molecular sieves.

**Equipment and Analysis.** The apparent molecular weight and molecular weight distributions were measured on a GPC system consisting of a Waters 510 HPLC pump, three Waters UltraStyragel columns (100, $10^3$, and $10^5$ Å), and a Waters 410 differential refractive index detector, with a DMF or THF flow rate of 1.0 mL/min. Poly(methyl methacrylate) was used as a calibration standard employing WinGPC software from Polymer Standards Service. $^1$H NMR spectra were collected in deuterated DMF or chloroform at 30 °C using a Bruker 300 MHz spectrometer. Monomer conversion was determined by gas chromatography (GC) using a Shimadzu GC 14-A gas chromatograph equipped with a FID detector and ValcoBond 30 m VB WAX Megabore column. Thermal characterization of the melt (mass ∼ 2−7 mg) was carried out using a differential scanning calorimeter (DSC 220) from Seiko Instruments, Inc., at a heating and cooling rate of 10 °C/min. The melting scan and temperature reported here are from the second heating run. Monolayer samples were prepared either by spin-casting using a Laurell Technologies Corp. spin-coater (model WS-400A-6NPP/Lite) or by Langmuir−Blodgett deposition using a KSV-5000 with Milli-Q double-distilled water as the subphase (18.2 MΩ·cm) onto mica substrates (Grade V-4 from SPI Supplier). Brush molecules were visualized using a multimode atomic force microscope from Veeco Metrology group equipped with Nanoscope IIIA control station and silicon cantilevers with resonance frequencies of about 160 kHz, spring constants of 5.0 N/m, and radii less than 10 nm. Custom computer software was used to obtain length measurements from the captured micrographs. Several images of ∼300 molecules were analyzed to ensure a standard error below 2% and an experimental error below 5% in average length measurements.

**Synthesis.** *Poly(2-hydroxyethyl methacrylate), PHEMA.* 0.014 g (0.1 mmol) of CuBr and 0.082 g (0.2 mmol) of dNbpy were added to a 25 mL Schlenk flask and degassed by vacuum followed by nitrogen backfill three times. Solvent (DMF; 5.0 mL) and HEMA (7.27 mL; 60 mmol) were degassed by bubbling with nitrogen for 30 min and then added to the Schlenk flask by syringe. An initial sample was taken by syringe, and then the initiator, EBiB (14.68 μL, 0.1 mmol), was added. The polymerization was conducted at 40 °C for 3 h. When monomer conversion reached 40%, the reaction was stopped by opening the flask to air, and the catalyst was removed by passing the solution through alumina. The polymer was obtained from the resulting reaction mixture by addition to THF to precipitate the solids which were filtered and dried under high vacuum at room temperature for 12 h. The isolated polymer was reprecipitated from DMF into THF three times and dried under vacuum at 25 °C for 24 h (DP of PHEMA = 240, as determined by GC). $M_n$(GPC) = 37 000 g/mol, $M_w/M_n$ = 1.26. $^1$H NMR (300 MHz, DMF-$d_7$, δ in ppm): 5.10 (1H, −COO−$CH_2$−$CH_2$−O*H*); 4.18 (2H, −COO−$CH_2$−$CH_2$−OH); 3.90 (2H, −COO−$CH_2$−$CH_2$−OH); 2.4−1.8 (2H, −[$CH_2$−C($CH_3$)]$_n$−); 1.25−0.95 (3H, −[$CH_2$−C($CH_3$)]$_n$−).

*Poly[{2-hydroxyethyl methacrylate}-block-{(2-(trimethylsilyloxy)-ethyl methacrylate}], PHEMA-b-PHEMATMS.* PHEMA with $M_n$(GPC) = 37 000 g/mol and $M_w/M_n$ = 1.26 (1.50 g, 0.05 mmol) and 0.042 g (0.1 mmol) of dNbpy were placed in a 25 mL Schlenk flask. The flask was sealed and purged with $N_2$ for 30 min. HEMATMS (6.0 g, 30 mmol) and dry DMF (3.0 mL) were degassed by bubbling with nitrogen for 30 min and then added to the Schlenk flask by syringe. An initial sample was taken by syringe, and then the catalyst, CuBr (7.0 mg, 0.05 mmol), was added. The polymerization was conducted at 80 °C for 16 h. When monomer conversion reached 80%, the reaction was stopped by opening the flask to air, and the catalyst was removed by passing the solution through alumina. The monomer and solvent were removed under high vacuum at 40 °C for 24 h to give the isolated block copolymer (DP of PHEMATMS = 480, as determined by GC). $M_n$(GPC) = 71 000 g/mol, $M_w/M_n$ = 1.45. $^1$H NMR (300 MHz, DMF-$d_7$, δ in ppm): 5.08 (1H, −COO−$CH_2$−$CH_2$−O*H*); 4.20 {(2H, −COO−$CH_2$−$CH_2$−OH), (2H, −COO−$CH_2$−$CH_2$−O−Si−($CH_3$)$_3$)}; 4.00 (2H, −COO−$CH_2$−$CH_2$−O−Si−($CH_3$)$_3$)); 3.90 (2H, −COO−$CH_2$−bp$CH_2$−OH); 0.33 (9H, −COO−$CH_2$−$CH_2$−O−Si−($CH_3$)$_3$)).

*Poly[{2-(2-bromoisobutyryloxy)ethyl methacrylate}-block-{(2-trimethylsilyloxy)ethyl methacrylate}], PBiBEM-b-PHEMATM.* A sample of PHEMA-*b*-PHEMATMS (0.35 g, assuming 0.654 mmol of OH groups) and DCC (0.25 g, 1.2 mmol) were placed in a 50 mL round-bottom flask. The flask was sealed and purged with $N_2$, and then 30 mL of methylene chloride was added. Then, 2-bromoisobutyric acid (0.2 g, 1.2 mmol) was added to the flask. The reaction mixture was stirred for 36 h at room temperature, and then the resulting reaction mixture was filtered and precipitated by addition to cold hexane. The precipitate was separated, redissolved in 10 mL of $CHCl_3$, reprecipitated into hexane, and dried under vacuum at room temperature for 24 h. $^1$H NMR confirmed complete conversion of the terminal OH groups to 2-bromoisobutyryl groups. $M_n$(GPC) = 58 000 g/mol, $M_w/M_n$= 1.54. $^1$H NMR (300 MHz, DMF-$d_7$, δ in ppm): 4.44 (2H, −COO−$CH_2$−$CH_2$−OOC−C($CH_3$)$_2$Br); 4.27 (2H, −COO−$CH_2$−$CH_2$−OOC−C($CH_3$)$_2$Br); 4.04 (2H, −COO−$CH_2$−$CH_2$−O−Si−($CH_3$)$_3$)); 3.83 (2H, −COO−$CH_2$−$CH_2$−O−Si−($CH_3$)$_3$)); 2.00 (6H, −COO−$CH_2$−$CH_2$−OOC−C-($CH_3$)$_2$Br); 0.17 (9H, −COO−$CH_2$−$CH_2$−O−Si−($CH_3$)$_3$)).

*Poly[{2-(2-bromoisobutyryloxy)ethyl methacrylate}-block-(2-hydroxyethyl methacrylate)], PBiBEM-b-PHEMA.* A sample of PBiBEM-*b*-PHEMATMS (0.1 g, assuming 0.3 mmol of TMS groups) was placed in a 50 mL round-bottom flask. The flask was sealed and purged with $N_2$, and then 30 mL of dry THF was added. Then, 1 mL of tetrabutylammonium fluoride (TBAF, 1.0 M in THF) was added to the flask. The reaction mixture was stirred for 2 h at room temperature while the resulting copolymer was precipitated gradually in THF. The precipitate was separated, washed with hexane, and dried under vacuum at room temperature for 24 h. $^1$H NMR confirmed complete conversion of the TMS groups to OH groups. $M_n$(GPC) = 79 000 g/mol, $M_w/M_n$ = 1.52. $^1$H NMR (300 MHz, DMF-$d_7$, δ in ppm): 5.63 (1H, −COO−$CH_2$−$CH_2$−O*H*); 4.61 (2H, −COO−$CH_2$−$CH_2$−OOC−C($CH_3$)$_2$Br); 4.44 (2H, −COO−$CH_2$−$CH_2$−OOC−C($CH_3$)$_2$Br); 4.18 (2H, −COO−$CH_2$−$CH_2$−OH); 3.90 (2H, −COO−$CH_2$−$CH_2$-OH); 2.17 (6H, −COO−$CH_2$−$CH_2$−OOC−C($CH_3$)$_2$Br).

*Poly[{2-(2-bromoisobutyryloxy)ethyl methacrylate}-block-{2-hydroxyethyl methacrylate-graft-(ε-caprolactone)], PBiBEM-b-(PHEMA-g-PCL).* A sample of PBiBEM-*b*-PHEMA with $M_n$(GPC) = 79 000 g/mol and $M_w/M_n$ = 1.22 (0.04 g, assuming 0.15 mmol of OH groups) was placed in a 25 mL Schlenk flask. The flask was sealed and purged with $N_2$ for 30 min. CL (1.05 g, 9.24 mmol) and dry DMF (2.0 mL) were added to the flask followed by a solution of $Sn(EH)_2$ (5.3 mg, 0.013 mmol) in dry DMF (1 mL). An initial sample was taken, and then the flask was placed in a thermostated oil bath at 110 °C. The polymerization was stopped after 30 h, exposed to air, and diluted with THF, and the PCL brush macromolecule was precipitated by addition of the solution to cold methanol. The solid polymer was dried under high vacuum ($DP_{sc}$ of CL = 30, as determined by NMR). $M_n$(GPC) = 1 200 000 g/mol, $M_w/M_n$ = 2.35. $^1$H NMR (300 MHz, $CDCl_3$, δ in ppm): 4.04 (2H, −[$CH_2$−$CH_2$−$CH_2$−$CH_2$−$CH_2$−OCO]$_n$−); 3.62 (2H, −OCO−$CH_2$−$CH_2$−$CH_2$−$CH_2$−$CH_2$−OH); 2.36 (2H, −[$CH_2$−$CH_2$−$CH_2$−$CH_2$−$CH_2$−OCO]$_n$−); 1.3−1.75 (6H, −[$CH_2$−$CH_2$−$CH_2$−$CH_2$−$CH_2$−OCO]$_n$−).

*Poly[{2-(2-bromoisobutyryloxy)ethyl methacrylate-graft-(n-butyl acrylate)}-block-{2-hydroxyethyl methacrylate-graft-(ε-caprolactone)],(PBiBEM-g-PBA)-b-(PHEMA-g-PCL).* A sample of PBiBEM-*b*-(PHEMA-*g*-PCL) (0.35 g, assuming 0.03 mmol of Br initiating groups), *n*-BA (3.1 g, 24 mmol), anisole (5.0 mL), and PMDETA (6.3 μL, 0.03 mmol) were added to a 10 mL Schlenk flask, and the reaction mixture was degassed by three freeze−pump−thaw cycles. Then, CuBr (0.0025 g, 0.03 mmol) was added under nitrogen. After stirring for 0.5 h at room temperature, the flask was placed in a

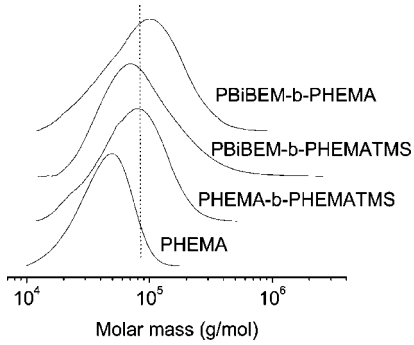


**Figure 1.** GPC traces of PHEMA, PHEMA-*b*-PHEMATMS, PBiBEM-*b*-PHEMATMS, and PBiBEM-*b*-PHEMA from GPC DMF line.

**Table 1. Synthesis of PBiBEM-*b*-PHEMA Block Copolymer Backbone**

| entry | DP | $M_{n,theory}{}^{c} \times 10^{-5}$ | $M_{n,app}{}^{d} \times 10^{-4}$ | $M_w/M_n{}^{d}$ |
|---|---|---|---|---|
| PHEMA | 240[a] | 3.1 | 3.7 | 1.26 |
| PHEMA-*b*-PHEMATMS | 240−480[b] | 12.8 | 7.1 | 1.45 |
| PBiBEM-*b*-PHEMATMS | 240−480 | 19.2 | 5.8 | 1.54 |
| PBiBEM-*b*-PHEMA | 240−480 | 12.9 | 7.9 | 1.52 |

[a] Calculated from conversion measured by gas chromatography. [b] Calculated from $^1$H NMR. [c] Calculated from conversion measured by gas chromatography assuming that polymer chains grow uniformly from the all initiating sites. [d] Apparent values determined by GPC in DMF with PMMA calibration.

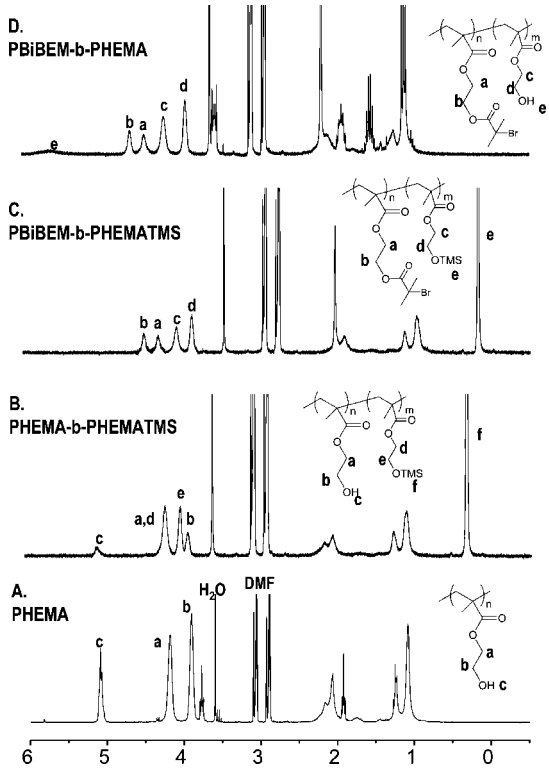


**Figure 2.** $^1$H NMR spectra (DMF-$d_7$) of (A) PHEMA, (B) PHEMA-*b*-PHEMATMS, (C) PBiBEM-*b*-PHEMATMS, and (D) PBiBEM-*b*-PHEMA.

preheated oil bath at 70 °C. The polymerization was stopped after 32 h by cooling the flask to room temperature and opening the flask to air. The resulting polymer solution was purified by passing through a column of neutral alumina. Then, the polymer was precipitated by adding the solution to methanol. The precipitate was separated, washed with methanol, and dried under vacuum at room temperature for 24 h ($DP_{sc}$ of *n*-BA = 90, as determined by NMR). $M_n$(GPC) = 1 700 000 g/mol, $M_w/M_n$ = 2.53. $^1$H NMR (300 MHz, $CDCl_3$, $\delta$ in ppm): 4.04 {(2H, $-[CH_2-CH_2-CH_2-CH_2-CH_2-OCO]_n-$), (2H, $-COO-CH_2-CH_2-CH_2-CH_3$)}; 2.32 {(2H, $-[CH_2-CH_2-CH_2-CH_2-CH_2-OCO]_n-$), (2H, $-[CH_2-CH]_n-$}; 0.91 (3H, $-COO-CH_2-CH_2-CH_2-CH_3$).

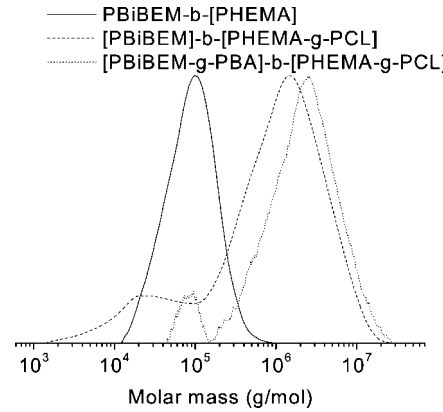


**Figure 3.** GPC traces of PBiBEM-*b*-PHEMA, PBiBEM-*b*-(PHEMA-*g*-PCL), and (PBiBEM-*g*-PBA)-*b*-(PHEMA-*g*-PCL) from GPC THF line.

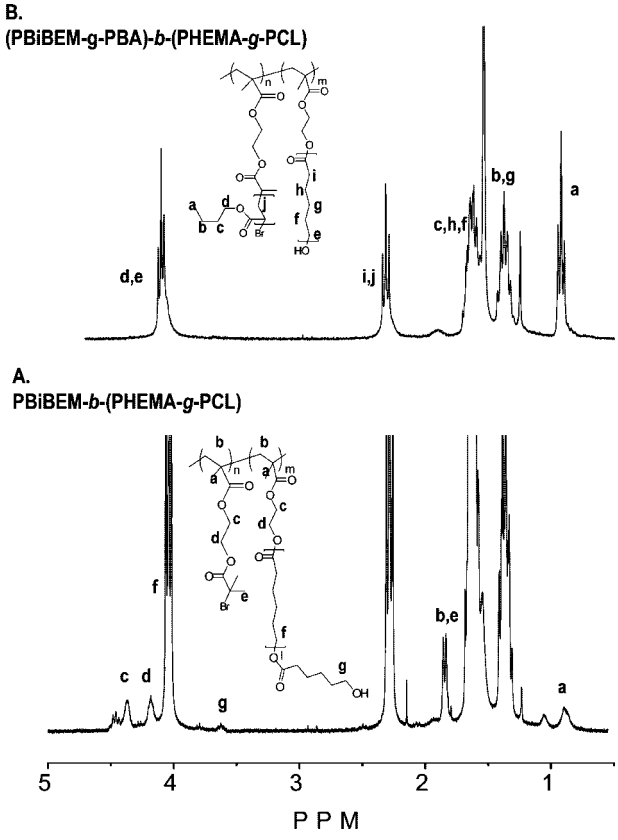


**Figure 4.** $^1$H NMR spectra ($CDCl_3$) of (A) PBiBEM-*b*-(PHEMA-*g*-PCL) and (B) (PBiBEM-*g*-PBA)-*b*-(PHEMA-*g*-PCL).

## Results and Discussion

The strategy employed in the synthesis of the hetero-grafted block brushes is illustrated in Scheme 2. ATRP and ROP were chosen as the polymerization mechanisms to independently grow PBA and PCL side chains, respectively. A well-defined block copolymer macroinitiator, PBiBEM-*b*-PHEMA, containing both bromine-containing ATRP initiating groups and hydroxyl-containing ROP initiating groups was prepared in four steps.

**Synthesis of Macroinitiators.** ATRP was used to directly prepare linear PHEMA with controlled molecular weight and

**Table 2. DSC Data for the Series of PCL-Containing Polymers[49,50]**

| | linear PCL ($n_{PCL} \cong 44$) | PCL brush ($n_{PCL} \cong 35$) | hetero-grafted brush ($n_{PCL} \cong 30$) | |
|---|---|---|---|---|
| | | | brush | $m_{PCL} = 0.36$ |
| $T_m$, °C | 53 | 53 | 54 | |
| $\Delta H_m$, J/g | 78 ± 2 | 72 ± 1 | 27 ± 4 | 75 ± 5 |
| $\Delta S_m$, J/(g K) | 0.24 ± 0.03 | 0.22 ± 0.01 | 0.08 ± 0.01 | 0.23 ± 0.02 |
| $T_c$, °C | 31 | 27 | 13 | |
| $\Delta H_c$, J/g | −79 ± 2 | −69 ± 1 | −20 ± 1 | −58 ± 2 |
| $\Delta S_c$, J/(g K) | −0.25 ± 0.03 | −0.23 ± 0.01 | −0.070 ± 0.01 | −0.20 ± 0.02 |
| $\chi_c$[a] | 0.58 ± 0.01 | 0.53 ± 0.01 | 0.20 ± 0.01 | 0.55 ± 0.01 |

[a] Degree of crystallinity, $\chi_c = \Delta H_m/\Delta H_m°$, $\Delta H_m° = 135$ J/g for PCL.[51]

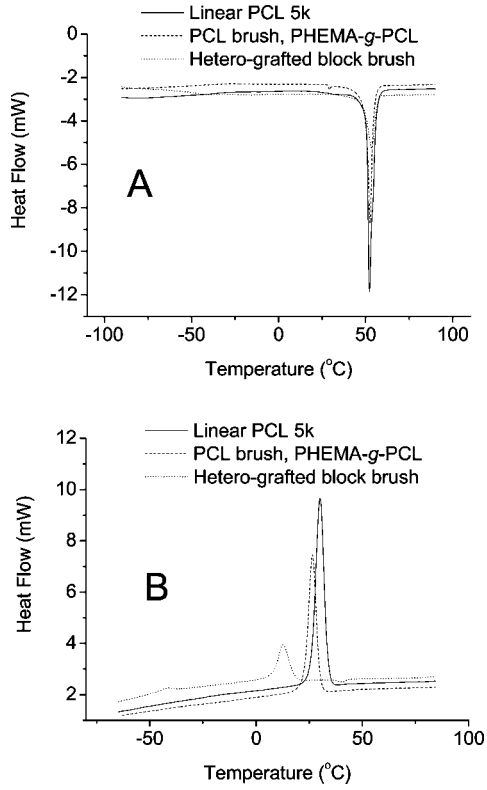


**Figure 5.** DSC Thermograms for the series of PCL-containing polymers. (A) The endothermic melting curves are very similar for the analyzed samples, exhibiting a sharp $T_m = 53-54$ °C. (B) However, for the exothermic crystallization curve, there is a definite downward shift in the $T_c$ of the hetero-grafted block brushes compared to the linear PCL and the PCL brushes. This is attributed to the hindered crystallization of the PCL block embedded in a matrix of PBA melt.

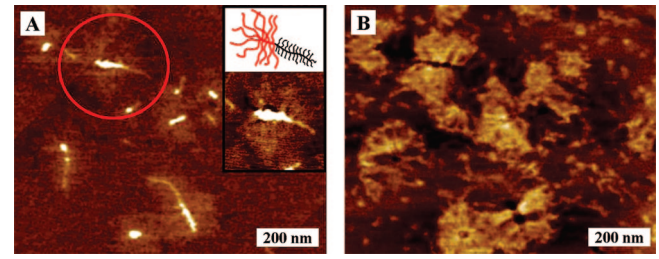


**Figure 6.** AFM images of single molecules of hetero-grafted block brushes. From the height image (A), one detects the presence of single brush molecules with a brighter PBA head and a less distinct PCL tail. Verification of the PBA and PCL assignment can be seen in the corresponding phase image (B). The PBA portion is wider than PCL side chains, which agrees with the NMR data. In addition, the contour length containing the PBA section appears to be shorter than that with PCL, again correlating with previous experimental results.

low polydispersity. DMF was used as a solvent, and a CuBr/dNbpy catalyst system was used for the homopolymerization of HEMA using ethyl 2-bromoisobutyrate (EBiB) as an initiator. The initial ratio of monomer to initiator was 600:1, and the polymerization was stopped when monomer conversion was 40% (DP = 240). The molecular weight and molecular weight distribution of the linear macroinitiator were obtained on a GPC DMF line using PMMA standards ($M_n$ = 37 000 g/mol, $M_w/M_n$ = 1.26) (Figure 1).

In the next step, PHEMA was used as a macroinitiator for chain extension with HEMATMS via ATRP. The reaction was carried out in DMF in the presence of a CuBr/dNbpy catalyst. DMF was chosen again as a solvent since both block segments are soluble in that solvent. The monomer conversion reached 80% after 16 h, and a copolymer, PHEMA-*b*-PHEMATMS, with $M_n$ = 71 000 g/mol and $M_w/M_n$ = 1.45, was obtained. GPC traces of the macroinitiator and resulting PHEMA-*b*-PHEMATMS block copolymer are shown in Figure 1. The results confirm the successful chain extension of PHEMA by HEMATMS with the GPC trace shifting to a higher molecular weight while retaining its symmetry. The polydispersity index increased slightly as PHEMA was chain extended to PHEMA-*b*-PHEMATMS, but overall the reaction occurred in a controlled manner. This block copolymer was analyzed by $^1$H NMR spectroscopy using DMF-$d_7$ as a solvent (Figure 2). In Figure 2B, new peaks, **e** and **f**, were detected in the NMR spectrum after chain extension to PHEMATMS. The integral ratio of peak **b** and **e** was 1:2, which was used to calculate the DP of PHEMATMS, DP = 480.

An esterification reaction was carried out in order to transform the −OH groups of PHEMA to bromoisobutyryl ATRP initiating groups. This was accomplished by reacting the PHEMA-*b*-PHEMATMS with 2-bromoisobutyric acid in methylene chloride using DCC as a coupling agent. The reaction conditions were mild enough to keep the −TMS groups intact. The GPC traces in Figure 1 show that the apparent molecular weight decreased after transformation from PHEMA-*b*-PHEMATMS to PBiBEM-*b*-PHEMATMS. This suggests that the hydrodynamic volume of PBiBEM is smaller than that of PHEMA.

The isolated block copolymer, PBiBEM-*b*-PHEMATMS, was further characterized by $^1$H NMR spectroscopy. The spectrum provides evidence of complete transformation of the terminal hydroxyl groups to the bromoisobutyryl ATRP initiating groups. After transformation to PBiBEM, the peak from the methylene protons adjacent to the hydroxyl group (peak **b** in Figure 2B) at 3.90 ppm disappeared while the new peaks, **a** and **b,** at 4.27 and 4.44 ppm (Figure 2C), which correspond to two methylene protons from PBiBEM, appeared as shown in Figure 2C, indicating a successful transformation.

The precursor backbone, PBiBEM-*b*-PHEMATMS, was easily transformed to a PBiBEM-*b*-PHEMA by treatment with tetrabutylammonium fluoride (TBAF) in THF. During the deprotection, the resulting macroinitiator, PBiBEM-*b*-PHEMA, was gradually precipitated in THF. It should be noted that the apparent molecular weight increased after deprotection from PBiBEM-*b*-PHEMATMS to PBiBEM-*b*-PHEMA (Figure 1), which is due to the greater hydrodynamic volume of PHEMA in DMF GPC. Overall high PDI of the macroinitiators estimated

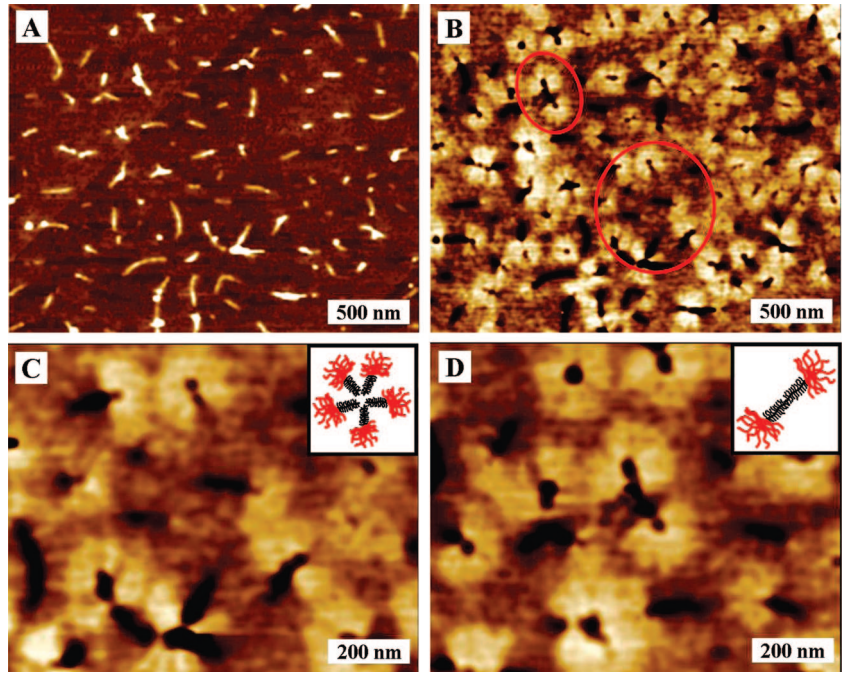


**Figure 7.** Height (A) and phase (B) AFM images of a dense film of the hetero-grafted block brushes. Similar to the images of single molecules in Figure 6, the corresponding phase image clearly demonstrates individual bottle-brush molecules with a bright and wide PBA head and a less distinct PCL tail. Furthermore, various association patterns, not seen in homopolymer brushes, are readily observed in the phase images of the dense film. For instance, some brushes form flower-like patterns (C) while some dumbbells are randomly scattered in the sample (D). These associations are attributed to the association/crystallization of the PCL blocks.

**Table 3. Results from Quantitative Analysis of the Hetero-Grafted PCL and PBA Block Brushes**

| | $L_n$, nm[a] | $l_m$, nm[b] | PDI[c] | $D$, nm[d] |
|---|---|---|---|---|
| PCL block | 110 ± 10 | 0.23 ± 0.02 | 1.25 ± 0.08 | 37 ± 3 |
| PBA block | 45 ± 4 | 0.19 ± 0.02 | 1.20 ± 0.07 | 120 ± 10 |
| whole brush | 160 ± 10 | 0.22 ± 0.02 | 1.16 ± 0.06 | |

[a] Number-average contour length. [b] Length per monomeric unit, $L_n/N_{backbone}$. [c] Polydispersity index, $L_w/L_n$. [d] Corona width.

by GPC can be due to poor compatibility of both blocks, since AFM analysis showed much lower PDI values for the final brushes (cf. below). $^1$H NMR spectroscopy (Figure 2D) showed that complete deprotection of the −TMS groups to hydroxyl groups was accomplished. A TMS peak at 0.17 ppm in Figure 2C completely disappeared while a broad peak of the hydroxyl groups at 5.63 ppm (Figure 2D) appeared, proving a successful deprotection.

**Synthesis of Hetero-Grafted Block Brushes by ROP and ATRP.** The hetero-grafted block brush with PCL and PBA side chains was synthesized in two steps using ROP followed by ATRP. ROP of caprolactone (CL) was initiated with the well-defined block copolymer backbone, PBiBEM-*b*-PHEMA macroinitiator. Polymerization was carried out at 1:2 ratio by volume of CL monomer in DMF with $Sn(EH)_2$ as a catalyst at 110 °C. Evidence of an increase in the molecular weight of the coil-*b*-brush copolymer, PBiBEM-*b*-(PHEMA-*g*-PCL), was provided by the complete shift of the GPC traces toward higher molecular weight (Figure 3). The small peak observed in the low molecular weight region of GPC traces indicates the presence of low molecular weight homopolymer/linear PCL, presumably initiated by traces of moisture or MeOH. In Figure 4A, the peaks **g** and **f** at 3.62 and 4.04 ppm represent the methylene protons adjacent to the terminal hydroxyl group and ester groups, respectively, from PBiBEM-*b*-(PHEMA-*g*-PCL). The integral ratio of these two peaks was used to obtain the DP of the PCL units, DP = 30.

Finally, in order to obtain a AB-type brush-*block*-brush copolymer, BA was grafted from the coil-*b*-brush copolymer, PBiBEM-*b*-(PHEMA-*g*-PCL), using the ATRP technique with [BA]:[PBiBEM-*b*-(PHEMA-*g*-PCL)]:[CuBr]:[PMDETA] = 800:1:1:1 at 70 °C in anisole. A conversion of 10% was obtained in 24 h, resulting in a (PBiBEM-*g*-PBA)-*b*-(PHEMA-*g*-PCL) brush-*block*-brush copolymer. After polymerization of BA, most of homo-PCL which was present in the reaction mixture was removed by precipitation into MeOH at room temperature while a (PBiBEM-*g*-PBA)-*b*-(PHEMA-*g*-PCL) was still soluble in MeOH due to the presence of the PBA segments. As shown in Figure 3, the GPC traces shifted slightly toward higher molecular weight after the polymerization of BA. A small low molecular weight peak was observed; the amount of homopolymer/linear PCL is small in comparison with the precursor macroinitiator, PBiBEM-*b*-(PHEMA-*g*-PCL). The subsequent AFM analysis provided more information on the molecular structure of hetero-grafted block brushes and also on their uniformity.

Successful polymerization of BA units was also confirmed by $^1$H NMR spectroscopy (Figure 4B) where two peaks at 4.04 and 0.91 ppm are observed. The ratio of integral between peak **a** and peak **d**, **e** is 0.9:1. Peak **a** originated from the terminal $-CH_3$ groups of PBA, and peaks **d** and **e** were contributions from the methylene group, $-[CH_2-CH_2-CH_2-CH_2-CH_2-OCO]_n-$, of PCL and from the methylene group, $-COO-CH_2-CH_2-CH_2-CH_3$, of PBA, respectively. Using these two peaks, the molar ratio between PCL and PBA was calculated to be 2:3. Finally, DP of PBA is calculated to be 90 since the backbone of the PCL part is twice longer than that of the PBA part. Thus, overall molecular formula of the hetero-grafted block brush is ($PBiBEM_{240}$-*g*-$PBA_{90}$)-*b*-($PHEMA_{480}$-*g*-$PCL_{30}$).

**Thermal Properties.** The thermal transitions of the hetero-grafted block brushes with PCL and PBA side chains, (PBiBEM-*g*-PBA)-*b*-(PHEMA-*g*-PCL), were investigated and compared to those of the PCL homopolymer brush (PHEMA-*g*-PCL) which was previously reported.[25] A summary of results is presented in Table 2, where linear PCL ($M_n \sim 5$K, $n_{PCL} \cong 44$) is included as a point of reference.

A melting transition at $T_m = 52.5 \pm 0.5$ °C was measured for both the homopolymer PCL and hetero-grafted block brushes (Figure 5A), which corresponds to about 50% crystallinity of the PCL domains.[48] In contrast to the nearly constant $T_m$, there was a distinct shift to a lower crystallization temperature $T_c$ upon addition of the amorphous PBA block (Figure 5B). One observes a significant drop in $T_c$ from the PCL brush ($T_c \cong 27$ °C) to the hetero-grafted block brush ($T_c \cong 13$ °C). This decrease in $T_c$ is ascribed to the hindered crystallization of the PCL sections covalently connected to the large and amorphous PBA block.

**AFM Characterization.** The success of the synthetic strategy for this complex hetero-grafted molecular brush was verified by atomic force microscopy (AFM). Clear imaging of individual brush molecules is facilitated by the adsorption of side chains which separate individual macromolecules and promote the extension of the backbone. In addition, the desorbed side chains increase the topographic contrast between the surface and the molecule by creating a distinctly delineated backbone.

Single molecule analysis of the complex bottle-brush architecture of the hetero-grafted brush was carried out. Figure 6 shows height and phase AFM images of a dilute film of the hetero-grafted block brush. In the height micrograph, one observes rodlike species that correspond to the PBA block, while the PCL section is barely visible. A stronger contrast between the two sections was achieved using AFM phase imaging due to significant difference in the viscoelastic properties of the liquid PBA and crystalline PCL. The PBA sections exhibited a wider corona and thicker backbone while the PCL block was noticeably thinner. Both observations are attributed to longer PBA side chains ($n_{PBA} \cong 90$ by NMR) compared to that of PCL ($n_{PCL} \cong 30$ by NMR). Adsorbed side chains result in the wide corona, while the desorbed side chains segregate at the backbone and accentuate the thickness increase.

Quantitative measurements were carried out using images obtained from a dense monolayer film of the hetero-grafted block brush (Figure 7). A summary of results is presented in Table 3. Similar to the dilute sample, the bottle-brushes have distinct head and tail regions corresponding to the PBA and the PCL blocks, respectively, that are distinguishable in phase images (Figure 7B). The contour length of the whole bottlebrush is $L_n = 160 \pm 10$ nm with a polydispersity index of PDI $= 1.16 \pm 0.06$. Given a total backbone degree of polymerization $N_b \cong 720$ (measured by NMR), the length per monomeric unit is $l_m = L_n/N_b = 0.22 \pm 0.02$ nm, indicating that the brushes are almost at full extension ($l_{max} \cong 0.25$ nm).[52] Because of the high imaging contrast, contour lengths and corona widths for the PBA and PCL sections were also independently determined. The PBA block with $N_{b,PBA} \cong 240$ has a number-average contour length of $L_n = 45 \pm 4$ nm (PDI $= 1.20 \pm 0.07$ and $l_m = 0.19 \pm 0.02$ nm). In the case of the PCL block with $N_{b,PCL} \cong 480$, one measures the $L_n = 110 \pm 10$ nm, PDI $= 1.25 \pm 0.08$, and $l_m = 0.23 \pm 0.02$ nm. These data indicate that both sections are fully extended.

The amphiphilic nature of the PCL and PBA brush blocks causes association of the diblock brushes, resulting in the various patterns observed in the phase images of the dense monolayers (Figure 7C,D).[53] Similar to the behavior of brush−coil block copolymers,[54] the micelle-like associations of these amphiphilic macromolecules are attributed to the microphase separation of the amorphous PBA side and the semicrystalline PCL. Note also that these macromolecules are rodlike and strongly anisometric (bulkier PBA section). This favors formation of circular aggregates (micelles) with a longer and thinner PCL block forming the core of the micelle (Figure 7C). In addition to the flower-like arrangement on the surface, one can also see simple dumbbell-like structures, which consist of two end-associating PCL chains (Figure 7D). These patterns are quite different from the stripes observed for the PHEMA-*g*-(PCL-*b*-PBA) brushes reported earlier wherein the PCL core blocks and amorphous PBA corona blocks formed herringbone stripes on the surface as the incompatible blocks can only microphase separate intramolecularly.[25]

## Conclusions

The combined ATRP and ROP methods were employed to prepare an AB-type hetero-grafted PBA brush-*block*-PCL brush copolymer by the entire "grafting from" approach. The well-defined PBiBEM-*b*-PHEMA block copolymer backbone, which possesses two distinct ATRP and ROP initiating groups, was successfully prepared in four steps. The crystalline PCL was synthesized by ROP from PBiBEM-*b*-PHEMA block copolymer backbone. Then, the amorphous PBA segments were synthesized by ATRP to give (PBiBEM-*g*-PBA)-*b*-(PHEMA-*g*-PCL). The DP of the PBiBEM-*b*-PHEMA backbone, the PCL side chain, and PBA side chain were 240−480, 30, and 90, respectively. DSC results showed that there is a significant drop in $T_c$ from the PCL brush to the hetero-grafted block brush, which is due to the frustrated crystalline packing of the PCL sections. A hetero-grafted PCL brush-*block*-PBA brush was directly visualized by AFM, which proved the successful synthesis of this complex molecule. From the AFM images, it was also seen that some of the brush molecules form a flower-like or dumbbell-like arrangement due to micelle-like association of the amphiphilic macromolecules.

**Acknowledgment.** This work was financially supported by the National Science Foundation (DMR 0606086, DMR 0549353, and CBET 0609087).

## References and Notes

(1) Beers, K. L.; Gaynor, S. G.; Matyjaszewski, K.; Sheiko, S. S.; Moeller, M. *Macromolecules* **1998**, *31*, 9413–9415.
(2) Dziezok, P.; Sheiko, S. S.; Fischer, K.; Schmidt, M.; Moller, M. *Angew. Chem., Int. Ed.* **1997**, *36*, 2812–2815.
(3) Ishizu, K. *Polym. J.* **2004**, *36*, 775–792.
(4) Wintermantel, M.; Gerle, M.; Fischer, K.; Schmidt, M.; Wataoka, I.; Urakawa, H.; Kajiwara, K.; Tsukahara, Y. *Macromolecules* **1996**, *29*, 978–983.
(5) Zhang, M.; Mueller, A. H. E. *J. Polym. Sci., Part A: Polym. Chem.* **2005**, *43*, 3461–3481.
(6) Sheiko Sergei, S.; Sun Frank, C.; Randall, A.; Shirvanyants, D.; Rubinstein, M.; Lee, H.-i.; Matyjaszewski, K. *Nature (London)* **2006**, *440*, 191–194.
(7) Djalali, R.; Li, S.-Y.; Schmidt, M. *Macromolecules* **2002**, *35*, 4282–4288.
(8) Zhang, M.; Estournes, C.; Bietsch, W.; Mueller, A. H. E. *Adv. Funct. Mater.* **2004**, *14*, 871–882.
(9) Zhang, M.; Teissier, P.; Krekhova, M.; Cabuil, V.; Mueller, A. H. E. *Prog. Colloid Polym. Sci.* **2004**, *126*, 35–39.
(10) Neugebauer, D.; Zhang, Y.; Pakula, T.; Sheiko, S. S.; Matyjaszewski, K. *Macromolecules* **2003**, *36*, 6746–6755.
(11) Pakula, T.; Zhang, Y.; Matyjaszewski, K.; Lee, H.-i.; Boerner, H.; Qin, S.; Berry, G. C. *Polymer* **2006**, *47*, 7198–7206.
(12) Matyjaszewski, K.; Xia, J. *Chem. Rev.* **2001**, *101*, 2921–2990.
(13) Wang, J.-S.; Matyjaszewski, K. *J. Am. Chem. Soc.* **1995**, *117*, 5614–5615.
(14) Matyjaszewski, K., Davis, T. P., Eds.; *Handbook of Radical Polymerization*; Wiley: Hoboken, NJ, 2002.
(15) Matyjaszewski, K. *Prog. Polym. Sci.* **2005**, *30*, 858–875.
(16) Braunecker, W. A.; Matyjaszewski, K. *Prog. Polym. Sci.* **2007**, *32*, 93–146.
(17) Matyjaszewski, K., Ed.; *Controlled/Living Radical Polymerization. From Synthesis to Materials*; ACS Symp. Ser. 944; American Chemical Society: Washington, DC, 2006.
(18) Matyjaszewski, K.; Qin, S.; Boyce, J. R.; Shirvanyants, D.; Sheiko, S. S. *Macromolecules* **2003**, *36*, 1843–1849.
(19) Boyce, J. R.; Shirvanyants, D.; Sheiko, S. S.; Ivanov, D. A.; Qin, S.; Boerner, H.; Matyjaszewski, K. *Langmuir* **2004**, *20*, 6005–6011.
(20) Khelfallah, N.; Gunari, N.; Fischer, K.; Gkogkas, G.; Hadjichristidis, N.; Schmidt, M. *Macromol. Rapid Commun.* **2005**, *26*, 1693–1697.

(21) Qin, S.; Matyjaszewski, K.; Xu, H.; Sheiko, S. S. *Macromolecules* **2003***36*, 605–612.
(22) Ishizu, K.; Satoh, J.; Sogabe, A. *J. Colloid Interface Sci.* **2004**, *274*, 472–479.
(23) Boerner, H. G.; Beers, K.; Matyjaszewski, K.; Sheiko, S. S.; Moeller, M. *Macromolecules* **2001**, *34*, 4375–4383.
(24) Cheng, G.; Boeker, A.; Zhang, M.; Krausch, G.; Mueller, A. H. E. *Macromolecules* **2001**, *34*, 6883–6888.
(25) Lee, H.; Jakubowski, W.; Matyjaszewski, K.; Yu, S.; Sheiko, S. S. *Macromolecules* **2006**, *39*, 4983–4989.
(26) Zhang, M.; Breiner, T.; Mori, H.; Muller, A. H. E. *Polymer* **2003**, *44*, 1449–1458.
(27) Lord, S. J.; Sheiko, S. S.; LaRue, I.; Lee, H.-i.; Matyjaszewski, K. *Macromolecules* **2004**, *37*, 4235–4240.
(28) Boerner, H. G.; Duran, D.; Matyjaszewski, K.; da Silva, M.; Sheiko, S. S. *Macromolecules* **2002**, *35*, 3387–3394.
(29) Lee, H.-i.; Matyjaszewski, K.; Yu, S.; Sheiko, S. S. *Macromolecules* **2005**, *38*, 8264–8271.
(30) Mecerreyes, D.; Jerome, R.; Dubois, P. *Adv. Polym. Sci.* **1999**, *147*, 1–59.
(31) Hashimoto, K. *Prog. Polym. Sci.* **2000**, *25*, 1411–1462.
(32) Stridsberg, K. M.; Ryner, M.; Albertsson, A.-C. *Adv. Polym. Sci.* **2002**, *157*, 41–65.
(33) Yamada, K.; Miyazaki, M.; Ohno, K.; Fukuda, T.; Minoda, M. *Macromolecules* **1999**, *32*, 290–293.
(34) Schappacher, M.; Deffieux, A. *Macromolecules* **2000**, *33*, 7371–7377.
(35) Neugebauer, D.; Theis, M.; Pakula, T.; Wegner, G.; Matyjaszewski, K. *Macromolecules* **2006**, *39*, 584–593.
(36) Neugebauer, D.; Zhang, Y.; Pakula, T.; Matyjaszewski, K. *Macromolecules* **2005**, *38*, 8687–8693.
(37) Neugebauer, D.; Zhang, Y.; Pakula, T.; Matyjaszewski, K. *Polymer* **2003**, *44*, 6863–6871.
(38) Neugebauer, D.; Sumerlin, B. S.; Matyjaszewski, K.; Goodhart, B.; Sheiko, S. S. *Polymer* **2004**, *45*, 8173–8179.
(39) Pietrasik, J.; Sumerlin, B. S.; Lee, R. Y.; Matyjaszewski, K. *Macromol. Chem. Phys.* **2007**, *208*, 30–36.
(40) Yamamoto, S.-i.; Pietrasik, J.; Matyjaszewski, K. *Macromolecules* **2007**, *40*, 9348–9353.
(41) Sun, F.; Sheiko, S. S.; Moeller, M.; Beers, K.; Matyjaszewski, K. *J. Phys. Chem. A* **2004**, *108*, 9682–9686.
(42) Potemkin, I. I.; Khokhlov, A. R.; Prokhorova, S.; Sheiko, S. S.; Moeller, M.; Beers, K. L.; Matyjaszewski, K. *Macromolecules* **2004**, *37*, 3918–3923.
(43) Sheiko, S. S.; Prokhorova, S. A.; Beers, K. L.; Matyjaszewski, K.; Potemkin, I. I.; Khokhlov, A. R.; Moeller, M. *Macromolecules* **2001**, *34*, 8354–8360.
(44) Sheiko, S. S.; da Silva, M.; Shirvaniants, D.; LaRue, I.; Prokhorova, S.; Moeller, M.; Beers, K.; Matyjaszewski, K. *J. Am. Chem. Soc.* **2003**, *125*, 6725–6728.
(45) Xu, H.; Shirvanyants, D.; Beers, K. L.; Matyjaszewski, K.; Dobrynin, A. V.; Rubinstein, M.; Sheiko, S. S. *Phys. Rev. Lett.* **2005**, *94*, 237801–237804.
(46) Matyjaszewski, K.; Patten, T. E.; Xia, J. *J. Am. Chem. Soc.* **1997**, *119*, 674–680.
(47) Pintauer, T.; Matyjaszewski, K. *Coord. Chem. Rev.* **2005**, *249*, 1155–1184.
(48) O'Leary, K. A.; Paul, D. R. *Polymer* **2006**, *47*, 1245–1258.
(49) Choi, J.; Kwak, S.-Y. *Macromolecules* **2004**, *37*, 3745–3754.
(50) Hu, H.; Dorset, D. L. *Macromolecules* **1990**, *23*, 4604–4607.
(51) Crescenzi, V.; Manzini, G.; Calzolari, G.; Borri, C. *Eur. Polym. J.* **1972**, *8*, 449–463.
(52) Sheiko, S. S.; Moeller, M. *Chem. Rev* **2001**, *101*, 4099–4123.
(53) Chen, H.-L.; Li, L.-J.; Ou-Yang, W.-C.; Hwang, J. C.; Wong, W.-Y. *Macromolecules* **1997**, *30*, 1718–1722.
(54) Neiser, M. W.; Muth, S.; Kolb, U.; Harris, J. R.; Okuda, J.; Schmidt, M. *Angew. Chem., Int. Ed.* **2004**, *43*, 3192–3195.

MA800412S